Domain-wall dynamics driven by thermal and electrical spin-transfer torque

Ya-Ru Wang [ORCID],[1] Chao Yang [ORCID],[2] Zheng-Chuan Wang [ORCID],[1,*] and Gang Su [ORCID][1,3,†]

[1]*School of Physical Sciences, University of Chinese Academy of Sciences, Beijing 100049, China*

[2]*College of Mechanical and Electrical Engineering, Wuyi University, Wuyishan 354300, Fujian, China*

[3]*Kavli Institute for Theoretical Sciences, CAS Center for Excellence in Topological Quantum Computation,*
University of Chinese Academy of Sciences, Beijing 100190, China

According to spin Seebeck effect, a thermal spin current will be produced when a temperature gradient is applied to the metallic ferromagnet. Similar to the electrical spin transfer torque (ESTT) induced by spin-polarized current, there is also a thermal spin transfer torque (TSTT) caused by the thermal spin current, which can be attributed to the *s-d* interaction between the conduction electrons and the local magnetization. In this paper, the generalized analytical expressions of thermal spin current and TSTT are derived based on the spinor Boltzmann equation (SBE) under the local equilibrium approximation. This generalized TSTT has different terms compared to the previous phenomenological form, and the phenomenological coefficients can be determined theoretically within our framework. Combined with the SBE under the applied electric field and temperature gradient, we solve the Landau-Lifshitz-Gilbert-Levy equation to study the domain wall (DW) motion driven by the ESTT and TSTT. We investigated the temperature-dependent DW motion, the total spin torque, and TSTT in permalloys. We found that the velocity of the DW can be promoted by increasing temperature and temperature gradient, which provide a path to effectively utilize the Joule heating in spintronics devices.

I. INTRODUCTION

Spintronics provides a feasible scheme for the development of nonvolatile, high-density, and high-speed memory devices. Since the discovery of the giant magnetoresistance effect [1] and spin transfer torque (STT) [2,3], magnetoresistance random access memory (MRAM) driven by spin-polarized current has been successfully developed and gradually realized industrially [4–7]. According to different driving mechanisms, MRAM can be classified as STT-MRAM [6,8] and SOT-MRAM; the latter use the spin-orbit torque (SOT) as the driving force [5,7,9–11]. In addition, the racetrack memory (RTM) based on the motion of a domain wall (DW) [12,13] and magnetic Skyrmion [14] driven by spin-polarized current has also attracted great interest from researchers. RTM is expected to become the latest generation of memory due to its advantages in size and energy consumption compared with MRAM. The writing operation of the above-mentioned memories is essentially carried out by switching the magnetization state with a high-intensity electrical current at least $10^5 \mathrm{A/cm}^2 \sim 10^7 \mathrm{A/cm}^2$ [15–17]. Because of this high current density, the significant rise in temperature due to the Joule heating effect may cause irreversible losses to the device, such as the reduction in lifetime and the degradation in the stability of the device. In other words, the difficulty in heat dissipation is one of the challenges faced by new magnetic memory devices. Therefore, to enhance the writing endurance, it is necessary to consider the thermal effects in the writing process in spintronics, that is to say, to develop the transport theory in the coupling case of charge, spin, and heat current, which gives birth to a developing branch of spintronics—spin caloritronics [18].

As early as 1987, Johnson *et al.* explored the dynamic laws for the simultaneous existence of charge, heat and spin current in magnetic metals [19]. In 2000, Wang *et al.* theoretically studied the spin-dependent thermoelectric transport in the spin valve structure [20]. In the latter, the discovery of spin Seebeck effect, which shows that the temperature gradient in a ferromagnet can induce a spin voltage or pure spin current [21,22], implies that there is a possibility to prolong the lifetime and improve the efficiency of magnetic memory device by rationally utilizing and controlling Joule heat. Since 2007, some theoretical calculations on the reversal of magnetization by heat currents in spin valves [23,24] have predicted the existence of spin heat accumulation and thermal spin transfer torque (TSTT) in the presence of temperature gradient. These predictions were experimentally confirmed by Yu *et al.* in the spin valve system of Co/Cu/Co [25]. At the same time, the role of temperature gradient on magnetic DWs also attracted extensive attention. Theoretically, the mechanism of temperature gradient-induced DW motion in magnetic nanowires was discussed by different methods [26–30]. Experimentally, Jiang *et al.* [31] directly observed the thermally driven DW motion in a magnetic insulator, and found that the DW "moves towards hot regime" when a temperature gradient is applied, and its velocity has a linear dependence on the temperature gradient. They proposed a magnonic STT mechanism to explain their observations, which is strong evidence for the existence of heat current-induced TSTT in continuous magnetic materials.

*wangzc@ucas.ac.cn

†gsu@ucas.ac.cn

Theoretical studies on DW motion driven by electrical spin transfer torque (ESTT) from spin-polarized current are mostly carried out by numerically solving the Landau-Lifshitz-Gilbert (LLG) equation involving the ESTT [32]. Similarly, exploiting the LLG equation containing TSTT to investigate the DW motion induced by TSTT from heat current will prove to be efficient. But the crucial point is how to accurately determine the expression of TSTT. In Refs. [26,28], based on the phenomenological ESTT in a static magnetization texture $\tau_c = -\frac{\hbar}{e}\frac{\gamma}{2AM_s}PG\Delta V(\frac{\partial \boldsymbol{M}}{\partial x} - \beta_c\boldsymbol{M}\times\frac{\partial \boldsymbol{M}}{\partial x})$ [33–36] (γ, M_s, and A are the gyromagnetic ratio, saturation magnetization and the cross section of magnetic nanowire, respectively, P is the spin polarization, G is the conductance, ΔV is the voltage gradient), this torque is caused by electrical spin current density $\boldsymbol{j}_c = \frac{\hbar}{e}\frac{\gamma}{2AM_s}PG\Delta V\boldsymbol{M}$, which simplifies the spin current as adiabatically following the local magnetization Ref. [33]. Bauer *et al.* phenomenologically introduced the expression of TSTT in a dynamic magnetization as $\tau_Q = -\frac{\hbar}{e}\frac{\gamma}{2AM_s}\frac{P'S}{\mathcal{L}T}J_Q(\frac{\partial \boldsymbol{M}}{\partial x} - \beta_Q\boldsymbol{M}\times\frac{\partial \boldsymbol{M}}{\partial x})$, where P' is called a spin conversion factor that converts the heat current J_Q into thermal spin current, S and $\mathcal{L}$ are the Seebeck coefficient and Lorenz number, respectively, J_Q stands for the heat current induced by the temperature gradient, and β_c and β_Q are called the β factors parametrizing the out-of-plane torque which is associated with ΔV and ΔT, respectively. Similar to phenomenological electrical spin current density $\boldsymbol{j}_c$, the thermal spin current density resulting in the above phenomenological τ_Q is approximated as $\boldsymbol{j}_Q = \frac{\hbar}{e}\frac{\gamma}{2AM_s}\frac{P'S}{\mathcal{L}T}J_Q\boldsymbol{M}$. It should be pointed out that the phenomenological material-dependent parameters P and P', β_c and β_Q need to be determined experimentally. To express the STT accurately, starting from the spinor Boltzmann equation (SBE), Wang rigorously derived the total spin torque in the presence of external field and temperature gradient, where the total spin torque contains both the ESTT and TSTT [37]. Based on Wang's method in Ref. [37], this paper simultaneously solves the SBE under an external electric field and a temperature gradient with the Landau-Lifshitz-Gilbert-Levy (LLGL) equation to explore thermally induced DW dynamics in a 1D magnetic nanowire with single DW. In addition to giving the analytical expression of TSTT, we systematically investigate the influence of temperature and temperature gradient on local magnetization, DW speed, and spin accumulation as well as the spin current of conduction electrons. The numerical results are comprehensive for us to enlighten how to take advantage of Joule heat in spin caloritronic devices.

This paper is organized as follows: In Sec. II, under the local equilibrium assumption, the spin diffusion equation satisfied by spin accumulation and spin current density is derived from SBE, which contain both the ESTT from bias and TSTT from temperature gradient. In Sec. III, as an example, we numerically solve both the SBE and LLGL equation in permalloy, where the ESTT and TSTT are considered. Finally, a summary and discussion is given in Sec. IV.

II. THEORETICAL FORMALISM

Consider a narrow 1D ferromagnetic metal wire with a single DW, as shown in Fig. 1. Driven by an external electric field E_x, the spin-polarized electrons by the left DW will move to the right, resulting in a STT. Besides, as described in
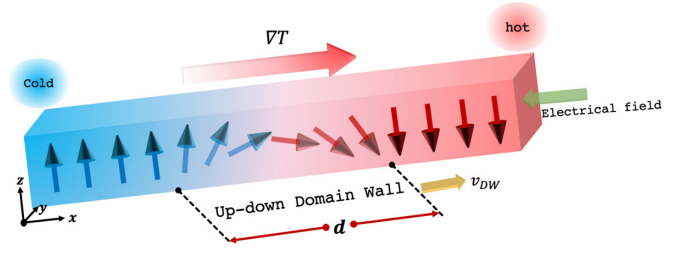

FIG. 1. The schematic structure of 1D ferromagnetic metal nanowire with a single DW in the presence of an $x-$ axis external electric field and a temperature gradient. The DW is a typical 180° Néel wall with width d. The magnetic domain on the left side of the DW is a pinnedlike layer which is used to polarize the spin of electrons. Under the drag force of spin torques induced by field and temperature gradient, the DW will move toward the right (hotter) end of the wire.

Ref. [21], the existence of spin Seebeck effect in ferromagnets will induce an additional pure spin current due to the temperature gradient. Therefore, the total spin torque applied to the DW are composed of ESTT from external electric field and TSTT from temperature gradient. To explore the expression of each torque, we take the SBE satisfied by the conduction electrons as the starting point [38],

$$\left(\frac{\partial}{\partial t} + \hat{v}_x\frac{\partial}{\partial x} - eE_x\frac{\partial}{\partial p}\right)\hat{f} + \frac{i}{\hbar}[\hat{\varepsilon}, \hat{f}] = -\left(\frac{\partial \hat{f}}{\partial t}\right)_{\text{collision}}, \quad (1)$$

where spinor distribution function $\hat{f}$ can be written as a 2×2 matrix $\hat{f} = \begin{pmatrix} f_{\uparrow\uparrow} & f_{\uparrow\downarrow} \\ f_{\downarrow\uparrow} & f_{\downarrow\downarrow} \end{pmatrix}$, the spinor energy is defined as $\hat{\varepsilon}(p) = \varepsilon(p)\hat{I} + \frac{1}{2}J_{\text{ex}}(p)\boldsymbol{M}(x,t)\cdot\hat{\boldsymbol{\sigma}}$, in which $J_{\text{ex}}(p)$ is the $s-d$ exchange coupling strength, $\boldsymbol{M}(x,t)$ represents the unit vector of magnetization in the DW, and $\hat{\boldsymbol{\sigma}}$ are the Pauli spin matrices. The spinor velocity $\hat{v}_x$ is

$$\hat{v}_x = \frac{\partial \hat{\varepsilon}}{\partial p} = \frac{\partial \varepsilon}{\partial p}\hat{I} + \frac{1}{2}\frac{\partial J_{\text{ex}}}{\partial p}\boldsymbol{M}\cdot\hat{\boldsymbol{\sigma}} = v_x\hat{I} + u_x\boldsymbol{M}\cdot\hat{\boldsymbol{\sigma}}, \quad (2)$$

where $v_x = \frac{\partial \varepsilon}{\partial p}$ and $u_x = \frac{1}{2}\frac{\partial J_{\text{ex}}}{\partial p}$.

Since any 2×2 matrix can be expanded using the complete basis $\{\hat{I}, \hat{\sigma}_x, \hat{\sigma}_y, \hat{\sigma}_z\}$, based on the local equilibrium assumption, we decompose the above $\hat{f}$ as the sum of the local equilibrium and nonequilibrium distribution function,

$$\hat{f}(p,x,t) = \hat{f}^0(p,x) + [f^1(p,x,t)\hat{I} + \boldsymbol{g}^1(p,x,t)\cdot\hat{\boldsymbol{\sigma}}], \quad (3)$$

where the local equilibrium distribution function adopt the form of diagonal matrix $\hat{f}^0(p,x) = \begin{pmatrix} f^0_{\uparrow\uparrow} & 0 \\ 0 & f^0_{\downarrow\downarrow} \end{pmatrix}$. For the ferromagnetic metal, the diagonal components are taken as the Fermi distribution function $f^0_{\uparrow\uparrow(\downarrow\downarrow)} = \{\exp[\frac{\varepsilon(p)\pm\frac{1}{2}J_{\text{ex}}-\mu(x)}{k_BT(x)}] + 1\}^{-1}$, where k_B is Boltzmann constant, μ is the chemical potential, and $\mu \approx E_F$ (Fermi energy) at finite temperature, the temperature distribution is simply chosen as $T(x) = T_0 + \kappa x$, which is linearly dependent on the position. By use of the above complete basis $\{\hat{I}, \hat{\sigma}_x, \hat{\sigma}_y, \hat{\sigma}_z\}$, we further expand $\hat{f}^0$ as $\hat{f}^0 = \frac{1}{2}(f^0_{\uparrow\uparrow} + f^0_{\downarrow\downarrow})\hat{I} + \frac{1}{2}(f^0_{\uparrow\uparrow} - f^0_{\downarrow\downarrow})\hat{\sigma}_z$. The scalar distribution function $f^1(p,x,t)$ and the vector distribution function $\boldsymbol{g}^1(p,x,t)$ in Eq. (3) are the distributions that deviate from local equilibrium, which correspond to

the charge distribution and spin distribution, respectively. For simplicity, we assume $F = \frac{1}{2}(f_{\uparrow\uparrow}^0 + f_{\downarrow\downarrow}^0) + f^1$ and $\boldsymbol{G} = \{g_x^1, g_y^1, \frac{1}{2}(f_{\uparrow\uparrow}^0 - f_{\downarrow\downarrow}^0) + g_z^1\}$, where we have rearranged the coefficients of $\{\hat{I}, \hat{\sigma}_x, \hat{\sigma}_y, \hat{\sigma}_z\}$ in Eq. (3) together. The collision term on the right side of Eq. (1) can be simplified in the relaxation time approximation as

$$\left(\frac{\partial \hat{f}}{\partial t}\right)_{\text{collision}} = \frac{F - \langle F \rangle}{\tau}\hat{I} + \frac{\boldsymbol{G} \cdot \hat{\boldsymbol{\sigma}} - \langle \boldsymbol{G} \cdot \hat{\boldsymbol{\sigma}} \rangle}{\tau_s}, \quad (4)$$

where τ and τ_s are the momentum and spin-flip relaxation time, respectively.

By substituting Eqs. (3) and (4) into Eq. (1), we can divide it into two equations, one is satisfied by the scalar distribution function F,

$$\left(\frac{\partial}{\partial t} + v_x \frac{\partial}{\partial x} - eE_x \frac{\partial}{\partial p}\right)F(p, x, t) + u_x \boldsymbol{M} \cdot \frac{\partial}{\partial x}\boldsymbol{G}(p, x, t)$$
$$= -\frac{F - \langle F \rangle}{\tau}, \quad (5)$$

and the other is satisfied by the vector distribution function $\boldsymbol{G}$,

$$\left(\frac{\partial}{\partial t} + v_x \frac{\partial}{\partial x} - eE_x \frac{\partial}{\partial p}\right)\boldsymbol{G}(p, x, t) - \frac{J_{\text{ex}}}{\hbar}\boldsymbol{M} \times \boldsymbol{G}(p, x, t)$$
$$+ u_x \boldsymbol{M} \frac{\partial}{\partial x}F(p, x, t) = -\frac{\boldsymbol{G} - \langle \boldsymbol{G} \rangle}{\tau_s}, \quad (6)$$

which are coupled together. By further expressing $\frac{\partial}{\partial x}\frac{1}{2}[f_{\uparrow\uparrow}^0(p, x) + f_{\downarrow\downarrow}^0(p, x)]$ and $\frac{\partial}{\partial x}\frac{1}{2}[f_{\uparrow\uparrow}^0(p, x) - f_{\downarrow\downarrow}^0(p, x)]$ in the above equations as

$$\frac{\partial}{\partial x}\frac{1}{2}[f_{\uparrow\uparrow}^0(p, x) + f_{\downarrow\downarrow}^0(p, x)]$$
$$= \frac{1}{2}\frac{\nabla T}{T}\left[\frac{1}{2}J_{\text{ex}}\left(\frac{\partial f_{\downarrow\downarrow}^0}{\partial \varepsilon} - \frac{\partial f_{\uparrow\uparrow}^0}{\partial \varepsilon}\right) - (\varepsilon - \mu)\left(\frac{\partial f_{\downarrow\downarrow}^0}{\partial \varepsilon} + \frac{\partial f_{\uparrow\uparrow}^0}{\partial \varepsilon}\right)\right] \quad (7)$$

and

$$\frac{\partial}{\partial x}\frac{1}{2}[f_{\uparrow\uparrow}^0(p, x) - f_{\downarrow\downarrow}^0(p, x)]$$
$$= \frac{1}{2}\frac{\nabla T}{T}\left[(\varepsilon - \mu)\left(\frac{\partial f_{\downarrow\downarrow}^0}{\partial \varepsilon} - \frac{\partial f_{\uparrow\uparrow}^0}{\partial \varepsilon}\right) - \frac{1}{2}J_{\text{ex}}\left(\frac{\partial f_{\downarrow\downarrow}^0}{\partial \varepsilon} + \frac{\partial f_{\uparrow\uparrow}^0}{\partial \varepsilon}\right)\right], \quad (8)$$

where

$$\left(-\frac{\partial f_{\uparrow\uparrow(\downarrow\downarrow)}^0}{\partial \varepsilon}\right) = \frac{1}{k_B T}\left\{\exp\left[\frac{\varepsilon(p) \pm \frac{1}{2}J_{\text{ex}} - \mu}{k_B T(x)}\right] + 1\right\}^{-1}$$
$$\times \left\{\exp\left[\frac{\mu - (\varepsilon(p) \pm \frac{1}{2}J_{\text{ex}})}{k_B T(x)}\right] + 1\right\}^{-1}, \quad (9)$$

it is obvious that the inhomogeneous terms in Eqs. (5) and (6) include the gradient of temperature ∇T, which causes the thermal spin current and heat current in the system.

According to the definition of charge density $n(x, t)$, charge current $j_e(x, t)$, spin accumulation $\boldsymbol{m}(x, t)$ and spin current density $\boldsymbol{j}_s(x, t)$ in Ref. [38],

$$n(x, t) = \int dp\, F(p, x, t), \quad (10)$$

$$j_e(x, t) = \int dp\, [v_x F(p, x, t) + u_x \boldsymbol{M} \cdot \boldsymbol{G}(p, x, t)], \quad (11)$$

$$\boldsymbol{m}(x, t) = \int dp\, \boldsymbol{G}(p, x, t), \quad (12)$$

and

$$\boldsymbol{j}_s(x, t) = \int dp\, [v_x \boldsymbol{G}(p, x, t) + u_x \boldsymbol{M} F(p, x, t)]. \quad (13)$$

By integrating over the variables p on both sides of Eqs. (5) and (6), we can obtain the continuity equation for charge density and charge current as

$$\frac{\partial}{\partial t}n(x, t) + \frac{\partial}{\partial x}j_e(x, t)$$
$$= -\frac{n - \langle n \rangle}{\tau} + \int dp\, u_x \frac{\partial \boldsymbol{M}}{\partial x} \cdot \boldsymbol{G}(p, x, t), \quad (14)$$

and the spin diffusion Eq. (15) for spin accumulation and spin current density as

$$\frac{\partial}{\partial t}\boldsymbol{m}(x, t) + \frac{\partial}{\partial x}\boldsymbol{j}_s(x, t)$$
$$= -\frac{\boldsymbol{m} - \langle \boldsymbol{m} \rangle}{\tau_{sf}} + \int dp\, u_x \frac{\partial \boldsymbol{M}}{\partial x}F(p, x, t) + \int dp\, \frac{J_{\text{ex}}}{\hbar}\boldsymbol{M}$$
$$\times \boldsymbol{G}(p, x, t). \quad (15)$$

In practical calculation, we often choose the s-d coupling strength J_{ex} and the spinor velocity u_x as constants. Therefore, the last two terms on the right side of Eq. (15) can be further written as $u_x n(x, t)\frac{\partial \boldsymbol{M}}{\partial x}$ and $\frac{J_{\text{ex}}}{\hbar}\boldsymbol{M} \times \boldsymbol{m}(x, t)$, while the latter is just the STT given by Levy *et al.* [39,40]. As we know, the system will arrive at a steady state after $t \gg \tau_s$ in the relaxation time approximation, so the time dependence of charge density, spin accumulation and spin current density can be expressed as $n(x, t) = \frac{1}{2}n(x)[1 + \exp(-\frac{t}{\tau})]$, $\boldsymbol{m}(x, t) = \frac{1}{2}\boldsymbol{m}(x)[1 + \exp(-\frac{t}{\tau_s})]$ and $\boldsymbol{j}_s(x, t) = \frac{1}{2}\boldsymbol{j}_s(x)[1 + \exp(-\frac{t}{\tau_s})]$, respectively, where $n(x)$, $\boldsymbol{m}(x)$ and $\boldsymbol{j}_s(x)$ are the charge density, spin accumulation and spin current density at the steady state, respectively. Substituting $n(x, t)$, $\boldsymbol{m}(x, t)$ and $\boldsymbol{j}_s(x, t)$ into Eq. (15), as detailed in the Appendix, we can obtain the spin accumulation $\boldsymbol{m}(x)$ at steady state as

$$\boldsymbol{m}(x) = \frac{1}{1 + \xi^2}\left\{\langle \boldsymbol{m} \rangle + \xi^2 \boldsymbol{M}\left[\boldsymbol{M} \cdot \langle \boldsymbol{m} \rangle - \tau_s \boldsymbol{M} \cdot \frac{\partial \boldsymbol{j}_s(x)}{\partial x}\right.\right.$$
$$+ \left.\tau_s u_x \boldsymbol{M} \cdot \frac{\partial \boldsymbol{M}}{\partial x}n(x)\right] - \frac{\tau_s}{1 + \xi^2}\left\{\frac{\partial \boldsymbol{j}_s(x)}{\partial x} + \xi \boldsymbol{M}\right.$$
$$\times \frac{\partial \boldsymbol{j}_s(x)}{\partial x} - u_x \frac{\partial \boldsymbol{M}}{\partial x}n(x) - \xi u_x \boldsymbol{M} \times \frac{\partial \boldsymbol{M}}{\partial x}n(x)\right\}, \quad (16)$$

where $\xi = \frac{J_{\text{ex}}}{\hbar}\tau_s$ is a dimensionless parameter.

According to the definition of STT $\tau_{\text{STT}} = \frac{J_{\text{ex}}}{\hbar}\boldsymbol{M} \times \boldsymbol{m}(x)$, the spin accumulation parallel to the background magnetization does not produce torque, so the terms $\frac{1}{1+\xi^2}\{\langle \boldsymbol{m} \rangle + \xi^2[\boldsymbol{M} \cdot \langle \boldsymbol{m} \rangle - \tau_s \boldsymbol{M} \cdot \frac{\partial}{\partial x}\boldsymbol{j}_s(x) + \tau_s u_x \boldsymbol{M} \cdot \frac{\partial \boldsymbol{M}}{\partial x}n(x)]\boldsymbol{M}\}$ in Eq. (16) does not contribute to the STT, which represent the adiabatic parts of spin accumulation, while the other terms in Eq. (16) that are not parallel to the local magnetization $\boldsymbol{M}$ represent

the nonadiabatic spin accumulation $\delta\boldsymbol{m}(x) = -\frac{\tau_s}{1+\xi^2}\{\frac{\partial \boldsymbol{j}_s(x)}{\partial x} + \xi\boldsymbol{M} \times \frac{\partial \boldsymbol{j}_s(x)}{\partial x} - u_x\frac{\partial \boldsymbol{M}}{\partial x}n(x) - \xi u_x\boldsymbol{M} \times \frac{\partial \boldsymbol{M}}{\partial x}n(x)\}$ which will have contribution to STT. Therefore, the total spin torque can be rewritten as

$$
\begin{aligned}
\boldsymbol{\tau}_{\text{total}} &= \frac{J_{\text{ex}}}{\hbar}\boldsymbol{M} \times \delta\boldsymbol{m}(x) \\
&= -\frac{\xi^2}{1+\xi^2}\left\{\frac{1}{\xi}\boldsymbol{M} \times \frac{\partial \boldsymbol{j}_s(x)}{\partial x} + \boldsymbol{M} \times \left[\boldsymbol{M} \times \frac{\partial \boldsymbol{j}_s(x)}{\partial x}\right]\right. \\
&\quad \left. -\frac{u_x}{\xi}\boldsymbol{M} \times \frac{\partial \boldsymbol{M}}{\partial x}n(x) - u_x\boldsymbol{M} \times \left[\boldsymbol{M} \times \frac{\partial \boldsymbol{M}}{\partial x}\right]n(x)\right\}.
\end{aligned}
\tag{17}
$$

The first two items in Eq. (17), which describe the spatial variation of spin current density, has usually been recognized as the source of spin torques, which has the same expression with Zhang's STT [41]. However, it is worth emphasizing that the spin current in this paper also includes the contribution caused by temperature gradient besides the contribution by electric field because the vector distribution function $\boldsymbol{G}(p, x, t)$ and scalar distribution function $F(p, x, t)$ in our spin current contain local equilibrium distribution function $\frac{1}{2}(f_{\uparrow\uparrow}^0 - f_{\downarrow\downarrow}^0)$ and $\frac{1}{2}(f_{\uparrow\uparrow}^0 + f_{\downarrow\downarrow}^0)$, which depend on $T(x)$ and will contribute the new temperature-dependent terms. Meanwhile, the spatial inhomogeneity of magnetization from the last two terms in Eq. (17) also contribute to STT. Similar to the first two terms, the last two items are also temperature dependent because they contain the local equilibrium distribution function $\frac{1}{2}(f_{\uparrow\uparrow}^0 + f_{\downarrow\downarrow}^0)$ in the scalar distribution function $F(p, x, t)$. By substituting $F(p, x, t)$ and $\boldsymbol{G}(p, x, t)$ into the definition of spin current Eq. (13), we could divide the total spin current into two parts $\boldsymbol{j}_s = \boldsymbol{j}_V + \boldsymbol{j}_T$, where $\boldsymbol{j}_T$ is the spin current generated by the temperature gradient with the components as follows:

$$
\begin{aligned}
j_{T_x} &= \int dp\, u_x M_x \frac{1}{2}(f_{\uparrow\uparrow}^0 + f_{\downarrow\downarrow}^0) = A(x)M_x(x, t), \\
j_{T_y} &= \int dp\, u_x M_y \frac{1}{2}(f_{\uparrow\uparrow}^0 + f_{\downarrow\downarrow}^0) = A(x)M_y(x, t), \\
j_{T_z} &= \int dp\left[v_x \frac{1}{2}(f_{\uparrow\uparrow}^0 - f_{\downarrow\downarrow}^0) + u_x M_z\frac{1}{2}(f_{\uparrow\uparrow}^0 + f_{\downarrow\downarrow}^0)\right] \\
&= A(x)M_z(x, t) + B(x),
\end{aligned}
\tag{18}
$$

where $A(x) = \frac{1}{2}\int dp\, u_x(f_{\uparrow\uparrow}^0 + f_{\downarrow\downarrow}^0)$ and $B(x) = \frac{1}{2}\int dp\, v_x(f_{\uparrow\uparrow}^0 - f_{\downarrow\downarrow}^0)$; they are all concerned with the

nonuniform temperature $T(x)$. $B(x)$ is usually smaller than $A(x)$, especially at high temperature, so the term $B(x)$ in $\boldsymbol{j}_T$ can be ignored, then the thermal spin current density in Eq. (18) can be approximated as $\boldsymbol{j}_T(x, t) \approx A(x)\boldsymbol{M}(x, t)$. Comparing it with the phenomenological thermal spin current density $\boldsymbol{j}_Q = \frac{\hbar}{e}\frac{\gamma}{2AM_s}\frac{S}{LT}P'J_Q\boldsymbol{M}$ in Ref. [26], we find the spin conversion factor can be determined as $P' = \frac{A(x)}{CJ_Q}$, where $C = \frac{\hbar}{e}\frac{\gamma}{2AM_s}\frac{S}{LT}$ is the constant in phenomenological spin current $\boldsymbol{j}_Q$. Different from the thermal spin current $\boldsymbol{j}_T$, $\boldsymbol{j}_V$ is the usual electrical spin current

$$
\boldsymbol{j}_V = \int dp\,[v_x\boldsymbol{g}^1(p, x) + u_x\boldsymbol{M}f^1(p, x)],
\tag{19}
$$

which is caused by the external electric field E_x. Similar to $\boldsymbol{j}_s$, the charge density n can also be divided into two terms $n_T + n_V$, in which the temperature-dependent charge density n_T can be written as

$$
n_T = \int dp\, \frac{1}{2}(f_{\uparrow\uparrow}^0 + f_{\downarrow\downarrow}^0),
\tag{20}
$$

and $n_V = \int dp\, f^1(p, x)$. Analogous to $\boldsymbol{j}_V$, the influence of temperature on n_V is much smaller than that of electric field.

Because the total spin current $\boldsymbol{j}_s$ and total charge density n can be decomposed into $\boldsymbol{j}_s = \boldsymbol{j}_V + \boldsymbol{j}_T$ and $n = n_V + n_T$, respectively, the total spin torque in Eq. (17) can be decomposed as $\boldsymbol{\tau}_{\text{total}} = \boldsymbol{\tau}_V + \boldsymbol{\tau}_T$, where the ESTT $\boldsymbol{\tau}_V$ is expressed as

$$
\begin{aligned}
\boldsymbol{\tau}_V &= -\frac{\xi^2}{1+\xi^2}\left\{\frac{1}{\xi}\boldsymbol{M} \times \frac{\partial \boldsymbol{j}_V(x)}{\partial x} + \boldsymbol{M} \times \left[\boldsymbol{M} \times \frac{\partial \boldsymbol{j}_V(x)}{\partial x}\right]\right. \\
&\quad \left. -\frac{u_x}{\xi}\boldsymbol{M} \times \frac{\partial \boldsymbol{M}}{\partial x}n_V(x) - u_x\boldsymbol{M} \times \left[\boldsymbol{M} \times \frac{\partial \boldsymbol{M}}{\partial x}\right]n_V(x)\right\}
\end{aligned}
\tag{21}
$$

and the TSTT $\boldsymbol{\tau}_T$ is expressed as

$$
\begin{aligned}
\boldsymbol{\tau}_T &= -\frac{\xi^2}{1+\xi^2}\left\{\frac{1}{\xi}\boldsymbol{M} \times \frac{\partial \boldsymbol{j}_T(x)}{\partial x} + \boldsymbol{M} \times \left[\boldsymbol{M} \times \frac{\partial \boldsymbol{j}_T(x)}{\partial x}\right]\right. \\
&\quad \left. -\frac{u_x}{\xi}\boldsymbol{M} \times \frac{\partial \boldsymbol{M}}{\partial x}n_T(x) - u_x\boldsymbol{M} \times \left[\boldsymbol{M} \times \frac{\partial \boldsymbol{M}}{\partial x}\right]n_T(x)\right\},
\end{aligned}
\tag{22}
$$

where the components of the spatial gradient of thermal spin current density $\frac{\partial \boldsymbol{j}_T}{\partial x}$ in $\boldsymbol{\tau}_T$ are

$$
\begin{aligned}
\frac{\partial j_{T_{x(y)}}}{\partial x} &= \frac{1}{2}\int dp\, u_x\left\{\frac{\partial M_{x(y)}}{\partial x}(f_{\uparrow\uparrow}^0 + f_{\downarrow\downarrow}^0) + M_{x(y)}\frac{\nabla T}{T}\left[\frac{1}{2}J_{\text{ex}}\left(\frac{\partial f_{\downarrow\downarrow}^0}{\partial\varepsilon} - \frac{\partial f_{\uparrow\uparrow}^0}{\partial\varepsilon}\right) - (\varepsilon - \mu)\left(\frac{\partial f_{\downarrow\downarrow}^0}{\partial\varepsilon} + \frac{\partial f_{\uparrow\uparrow}^0}{\partial\varepsilon}\right)\right]\right\}, \\
\frac{\partial j_{T_z}}{\partial x} &= \frac{1}{2}\int dp\left\{\left[\frac{1}{2}u_x M_z J_{\text{ex}} + v_x(\varepsilon - \mu)\right]\left(\frac{\partial f_{\downarrow\downarrow}^0}{\partial\varepsilon} - \frac{\partial f_{\uparrow\uparrow}^0}{\partial\varepsilon}\right) - \left[u_x M_z(\varepsilon - \mu) + \frac{1}{2}v_x J_{\text{ex}}\right]\left(\frac{\partial f_{\downarrow\downarrow}^0}{\partial\varepsilon} + \frac{\partial f_{\uparrow\uparrow}^0}{\partial\varepsilon}\right)\right\}\frac{\nabla T}{T} \\
&\quad + \frac{1}{2}\int dp\, u_x\frac{\partial M_z}{\partial x}(f_{\uparrow\uparrow}^0 + f_{\downarrow\downarrow}^0).
\end{aligned}
\tag{23}
$$

Equation (23) suggests that the TSTT is proportional to $\frac{\nabla T}{T}$. Focusing on the first two terms in $\boldsymbol{\tau}_T$ with temperature gradient $\frac{\partial T}{\partial x}$, i.e., the fieldlike or out-of-plane thermal torque, $\boldsymbol{\tau}_{fl} = -\frac{\xi}{1+\xi^2}\boldsymbol{M} \times \frac{\partial \boldsymbol{j}_T(x)}{\partial x}$, and the dampinglike or in-plane thermal torque: $\boldsymbol{\tau}_{dl} = -\frac{\xi^2}{1+\xi^2}\boldsymbol{M} \times [\boldsymbol{M} \times \frac{\partial \boldsymbol{j}_T(x)}{\partial x}]$, which are related to $\frac{\partial \boldsymbol{j}_T(x)}{\partial x}$ in Eq. (22). If we rewrite the dampinglike thermal torque in Eq. (22)

as $\boldsymbol{\tau}_{\mathrm{dl}} = -\frac{\xi^2}{1+\xi^2}[(\boldsymbol{M} \cdot \frac{\partial \boldsymbol{j}_T(x)}{\partial x})\boldsymbol{M} - \frac{\partial \boldsymbol{j}_T(x)}{\partial x}]$, then the first two terms in Eq. (22) can be re-expressed as

$$\frac{\xi^2}{1+\xi^2}\frac{\partial \boldsymbol{j}_T(x)}{\partial x} - \frac{\xi}{1+\xi^2}\boldsymbol{M} \times \frac{\partial \boldsymbol{j}_T(x)}{\partial x} - \frac{\xi^2}{1+\xi^2}\left(\boldsymbol{M} \cdot \frac{\partial \boldsymbol{j}_T(x)}{\partial x}\right)\boldsymbol{M}. \tag{24}$$

Comparing Eq. (24) with Bauer's phenomenological TSTT $\boldsymbol{\tau}_Q = \frac{\partial \boldsymbol{j}_Q}{\partial x} - \beta_Q \boldsymbol{M} \times \frac{\partial \boldsymbol{j}_Q}{\partial x}$ in Ref. [26], where $\boldsymbol{j}_Q = CP'J_Q\boldsymbol{M}$ is the density of thermal spin current, we find they are similar except for the third term in our expression, although the two expressions of the thermal spin current are different, where our thermal spin current $\boldsymbol{j}_T$ is derived from SBE, which is more complicated than the phenomenological expression $\boldsymbol{j}_Q$. For the dampinglike term $\boldsymbol{\tau}_{\mathrm{dl}}$ in Eq. (24) with in-plane torque $\frac{\partial \boldsymbol{j}_Q}{\partial x}$ in Bauer's equation, we find that both of them originate from the spatial gradients of the thermal spin current. However, referring to Slonczewski's STT in magnetic multilayers [2] and Zhang-Li's STT in continuous micromagnetic structures [33], we believe that only the transverse component which is perpendicular to magnetization in dampinglike torque can contribute to the in-plane torque. Therefore, the third term in Eq. (24) has no contribution to the TSTT and can be neglected, then the dampinglike thermal torque will reduce to the Bauer's expression, in which the gradient of the thermal spin current is just perpendicular to the magnetization. Focusing on the out-of-plane TSTT $\frac{\xi}{1+\xi^2}\boldsymbol{M} \times \frac{\boldsymbol{j}_T}{\partial x}$ in Eq. (24) and $\beta_Q \boldsymbol{M} \times \frac{\boldsymbol{j}_Q}{\partial x}$ in $\boldsymbol{\tau}_Q$, the phenomenological β_Q factor can be determined by

$$\beta_Q = \frac{\xi}{1+\xi^2}, \tag{25}$$

which depends on the exchange coupling strength J_{ex} and spin-flip relaxation time τ_s. Besides the first two terms in Eq. (22), the TSTT in our paper also contains more new terms (the third and fourth terms) than the phenomenological TSTT, and they are contributed by the charge density, which is $T(x)$ dependent. It should be noted that the TSTT in Eq. (22) is strictly derived from the SBE of spin-polarized electron, so it is more accurate and suitable for the study of magnetization dynamics driven by thermal and electrical spin currents.

Driven by ESTT and TSTT, the motion of magnetization in the DW follows the LLG equation including the total spin torque in Eq. (17), which is called the LLGL equation,

$$\frac{\partial \boldsymbol{M}(x,t)}{\partial t} = -\gamma \boldsymbol{M}(x,t) \times \boldsymbol{H}_{\mathrm{eff}} + \frac{\alpha}{M_s}\boldsymbol{M}(x,t) \times \frac{\partial \boldsymbol{M}(x,t)}{\partial t}$$
$$- \frac{J_{\mathrm{ex}}}{\hbar}\boldsymbol{M}(x,t) \times \boldsymbol{m}(x), \tag{26}$$

where α is the Gilbert damping coefficient. $\boldsymbol{H}_{\mathrm{eff}}$ in the first term is the effective field, which usually includes anisotropy field, exchange coupling field between spins on neighboring magnetization, external magnetic field, and demagnetizing field. The second term describes the effect of magnetic damping on the precession of magnetization. The third term is the Levy's STT which contains both electrical and thermal STT given in Eqs. (21) and (22), respectively. Obviously, it

is impossible to know the motion of magnetization in the DW by solving Eq. (26) alone. The appropriate and accurate treatment is to solve the coupled equations SBE + LLGL simultaneously, that is, the SBE Eqs. (5) and (6) satisfied by the spin-polarized electron and the LLGL Eq. (26) satisfied by the local magnetization. The numerical results of Eqs. (5), (6), and (26) are shown in the next section.

III. NUMERICAL RESULTS

Due to the complexity of the coupled partial differential Eqs. (5), (6), and (26), we need to make some appropriate approximations before numerical calculation. First, Eqs. (5) and (6) can be simplified to the SBE at the steady state after the relaxation time, which means the scalar and vector distribution function satisfy $\frac{\partial F(p,x,t)}{\partial t} = 0$ and $\frac{\partial \boldsymbol{G}(p,x,t)}{\partial t} = 0$. Since the speed of conduction electrons are much faster than the motion of local magnetization, the momentum and spin relaxation time τ and τ_s are much smaller than that of the local magnetization, meaning that the charge and spin redistribution of polarized electrons occur much faster than the motion of background magnetization. In other words, we first assume that the charge density and spin density for the electrons have reached a quasisteady state before the magnetization starts to move, then we substitute the quasisteady solution into the total spin torque in Eq. (26) and solve it. For simplicity, the complex effective field in Eq. (26) is simplified to the magnetization at the initial time $\boldsymbol{H}_{\mathrm{eff}}(x,t) = c\boldsymbol{M}(x,0)$, where c is a constant, which is convenient for us to study the effect of total spin torque in DW motion. The initial state of magnetization inside the DW is chosen as $\boldsymbol{M}(x,0) = M_s(\cos\theta, 0, \sin\theta)$, where $\theta = \frac{\pi}{2} - \frac{x}{d}\pi$. The equilibrium scalar distribution function in Eq. (5) is adopted as $\langle F \rangle = \frac{1}{2}(f_{\uparrow\uparrow}^0 + f_{\downarrow\downarrow}^0)$ and the equilibrium vector distribution function in Eq. (6) is taken as $\langle \boldsymbol{G} \rangle = \exp(i\frac{J_{\mathrm{ex}}}{\hbar v_x}x)\boldsymbol{M}(x,t)$ [40]. The boundary conditions for the distribution function are taken as $\begin{cases} F(p,x_{\min}) = \langle F \rangle(p,x_{\min}) \\ F(p_{\min},x) = \langle F \rangle(p_{\min},x) \end{cases}$ and $\begin{cases} \boldsymbol{G}(p,x_{\min}) = \langle \boldsymbol{G} \rangle(p,x_{\min}) \\ \boldsymbol{G}(p_{\min},x) = \langle \boldsymbol{G} \rangle(p_{\min},x). \end{cases}$ The differential Eqs. (5), (6), and (26) are solved by the difference method and the procedure is briefly described as follows: (1) Substituting the initial magnetization $\boldsymbol{M}(x,0)$ into the SBEs (5) and (6) for the spin-polarized electrons, the spinor distribution function of the polarized electrons at the initial times $F(p,x,0)$ and $\boldsymbol{G}(p,x,0)$ can be obtained. According to the definition of spin accumulation Eq. (12) and spin current density Eq. (13), it is easy to get the initial spin accumulation $\boldsymbol{m}(x,0)$ and the initial spin current density $\boldsymbol{j}_s(x,0)$ by integrating $F(p,x,0)$ and $\boldsymbol{G}(p,x,0)$ over the momentum. (2). Substituting the $\boldsymbol{m}(x,0)$ obtained in the first step back into the LLGL equation of magnetization and solving Eq. (26) numerically by the difference method, the magnetization at the next time $\boldsymbol{M}(x,0+\Delta t)$ driven by total spin torque which contains both the TSTT and ESTT can be obtained. Repeat the above two steps until the system, i.e.,

TABLE I. The physical constants and parameters in our paper.

Physical constants/parameters	Symbol	Value	Unit
Gyromagnetic ratio	γ	2.21×10^5	$\frac{m}{A \cdot s}$
Saturation magnetization	M_s	8×10^5	$\frac{A}{m}$
Momentum relaxation time of electron	τ	1×10^{-15}	s
Spin-flip relaxation time of electron	τ_{sf}	1×10^{-12}	s
Fermi energy	E_F	0.14	eV
Fermi velocity	v_F	2.21×10^5	$\frac{m}{s}$
s-d exchange coupling strength	J_{ex}	0.106	eV
Spinor velocity	u_x	1.93×10^5	$\frac{m}{s}$
Width of DW	d	5	nm
Electrical field	E_x	-8×10^3	$\frac{V}{m}$
Electrical conductivity	σ	1.26×10^6	$\frac{1}{\Omega \cdot m}$
Damping parameter	α	0.2	

magnetization inside the DW and spin accumulation of electrons, reaches the final steady state. The physical constant and parameters are listed in Table I, where we adopt the materials parameters for permalloy. Based on the above approximation, Eqs. (5), (6), and (26) are solved simultaneously. The numerical results for the physical quantities including magnetization inside the DW $\boldsymbol{M}(x, t)$, spin accumulation $\boldsymbol{m}(x, t)$ of electrons, total spin torque $\boldsymbol{\tau}_{\mathrm{total}}$, and TSTT $\boldsymbol{\tau}_T$ are shown below. Section III A concentrates on the magnetization dynamics at different temperature gradients $\kappa = \nabla T$ and Sec. III B focuses on the characters of physical quantities at different cold end temperature T_0.

A. Magnetization dynamics at different temperature gradients κ

By numerically solving the equations SBE + LLGL simultaneously, the motion of magnetization $\boldsymbol{M}(x, t) = (M_x, M_y, M_z)$ and spin accumulation $\boldsymbol{m}(x, t) = (m_x, m_y, m_z)$ inside the DW driven by both ESTT and TSTT can be obtained directly. In this subsection, we take the electric field as $E_x = -8 \times 10^3$ V/m, the temperature at cold port as $T_0 = 100$ K. As shown in Fig. 2, the vector of local magnetization $\boldsymbol{M}(x, t)$ (green arrows) and spin accumulation $\boldsymbol{m}(x, t)$ (red arrows) at each position for different times is intuitively displayed. At the initial time, the magnetization inside the DW is $\boldsymbol{M}(x, 0)$, which has a different direction with the spin accumulation obtained by calculating SBE. Then the total spin torque $\boldsymbol{\tau}_{\mathrm{total}} = \frac{J_{\mathrm{ex}}}{\hbar} \boldsymbol{M} \times \boldsymbol{m}$ caused by the field and the temperature gradient is applied to change the direction of both $\boldsymbol{M}(x, t)$ and $\boldsymbol{m}(x, t)$. After ~ 0.15 ns, the magnetization and spin accumulation tend to be parallel $\boldsymbol{M} \parallel \boldsymbol{m}$ and finally reach the steady state together, then $\frac{\partial \boldsymbol{M}(x, t)}{\partial t} = 0$ and $\frac{\partial \boldsymbol{m}(x, t)}{\partial t} = 0$. In the steady state, the direction of magnetization inside the DW is the same as that of the left domain in Fig. 1, which means that the left domain has moved to the position of the original DW and the DW has completely slipped to the right (hot) end after 0.15 ns. If the time for the system to reach the steady state is t_s, then the velocity of DW can be estimated as $v_{\mathrm{DW}} = \frac{d}{t_s}$, where d is the width of the DW. In this subsection, we fixed the cold end temperature at $T_0 = 100$ K and calculated the magnetization and spin accumulation in DW at the temperature gradients $\kappa = 0.5$ K/nm, 1 K/nm, 2 K/nm, 4 K/nm, 6 K/nm, respectively.
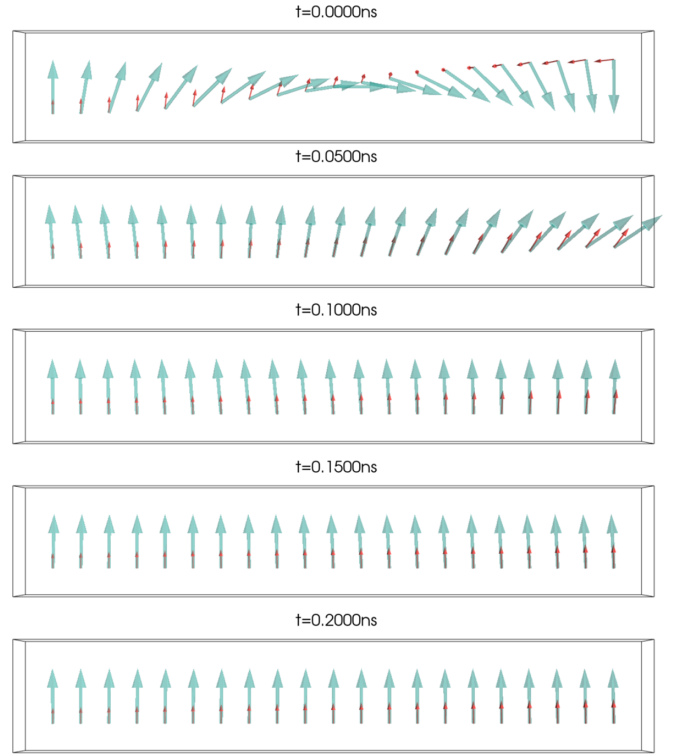

FIG. 2. The 3D vector diagram of magnetization $\boldsymbol{M}(x, t)$ (marked by green arrow) and spin accumulation $\boldsymbol{m}(x, t)$ (indicated by red arrow). The temperature gradient are taken as $\kappa = 2$ K/nm.

Their magnetization dynamics are displayed in Fig. S1 in the Supplemental Material [42]. From Fig. S1, it can be directly seen that the larger the temperature gradient κ, the faster the DW motion. In Fig. 3, we plot the total magnetic moment $\langle \boldsymbol{M} \rangle = \int_0^d \boldsymbol{M}(x, t) \, dx$ versus time at different κ, from which we can simply determine the time t_s for the system to stabilize, that is, the time for the DW to slide to the right end. For instance, for the maximum temperature gradient $\kappa = 6$ K/nm, t_s is ~ 0.08 ns, and $v_{\mathrm{DW}} \approx 62.5$ m/s, while for the minimum temperature gradient $\kappa = 0.5$ K/nm, the magnetization takes 0.23 ns to reach the steady state and $v_{\mathrm{DW}} \approx 21.7$ m/s, which is much slower than that at $\kappa = 6$ K/nm. Experimentally, it is widely observed that the velocity of the DWs increases with the increasing ∇T, both in ferromagnetic materials [43,44] and in magnetic insulators [31]. The thermal drag force induced by ∇T comes from the angular-momentum driving force [29,30]. In magnetic metals, the force is called TSTT, which is the angular momentum transfer between thermal spin current generated by ∇T and DW, while in magnetic insulators, it is inferred as magnonic STT [30,31], which comes from the angular momentum transfer between spin-wave (magnon) spin current caused by the spin-wave Seebeck effect [45] and DWs. For magnetic conductors, we derive a more rigorous analytical expression of TSTT than that proposed phenomenologically, and its variation with ∇T is consistent with the experimental phenomenon, as shown in Fig. 4.

Once the coupling equations SBE + LLGL Eqs. (5), (6), and (26) are solved numerically, we can also obtain the thermal spin current density $\boldsymbol{j}_T$ defined by Eq. (18) and the total
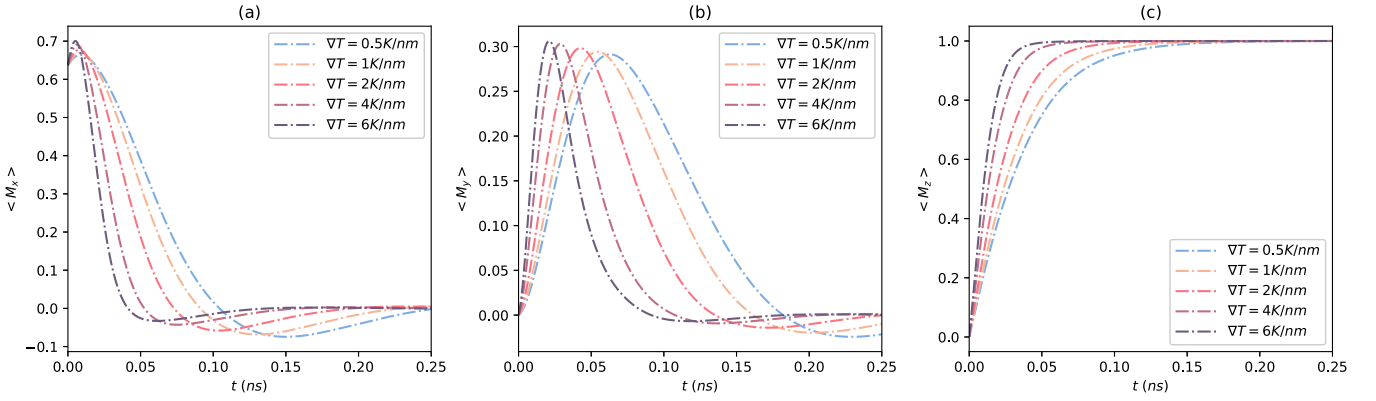
FIG. 3. The $x-$, $y-$, $z-$ component of the total magnetic moment $\langle \boldsymbol{M} \rangle (t)$ at different temperature gradients versus time.

spin current density $\boldsymbol{j}_s$ defined by Eq. (13), where $\boldsymbol{j}_s$ is the sum of electrical spin current density $\boldsymbol{j}_V$ and thermal spin current density $\boldsymbol{j}_T$. By inserting $\boldsymbol{j}_s$ into Eq. (17) and $\boldsymbol{j}_T$ into Eq. (22), the variation of total spin torque $\boldsymbol{\tau}_{\text{total}}$ and TSTT $\boldsymbol{\tau}_T$ with position x at different times can be calculated accordingly. We have shown $\boldsymbol{\tau}_{\text{total}}$ and $\boldsymbol{\tau}_T$ at the initial time $t = 0$ in Fig. 4, which implies that both the total spin torque and the TSTT increase with the temperature gradient. The TSTT increases because it is proportional to the temperature gradient ∇T according to Eq. (23), while the total spin torque increases due to the TSTT. By comparing the total spin torque $\boldsymbol{\tau}_{\text{total}}$ and TSTT $\boldsymbol{\tau}_T$ at a time under a certain ∇T in Fig. 4, we can find that the TSTT is more than half of the total spin torque, which indicates that the TSTT induced by a temperature gradient is greater than the ESTT induced by the electric field 8×10^3 V/m (or electrical current 10^6 A/cm^2 for a permalloy with conductivity $1.26 \times 10^6 \, \Omega^{-1} \text{m}^{-1}$).

B. Magnetization dynamics at different cold end temperature T_0

In this subsection, we will show the influence of different cold end temperature T_0 on various physical quantities; here we adopt the electric field as $E_x = -8 \times 10^3$ V/m, the temperature gradient as $\kappa = 5$ K/nm. In Fig. 5, the magnetization $\boldsymbol{M}(x)$ and spin accumulation $\boldsymbol{m}(x)$ versus position at time $t = 0.05$ ns for different cold end temperatures $T_0 = 150$ K, 175 K, 200 K, 225 K, 250 K are shown. The dynamics is given in Fig. S2 in Supplemental Material. From Fig. S2, it is easy to find that the higher the cold end temperature T_0, the larger the spin accumulation and the faster the DW moves. Similar to Fig. 3, Fig. 6 shows the total magnetic moment $\langle \boldsymbol{M} \rangle (t)$ at different cold end temperatures, from which the velocity of DW motion can be evaluated, which accelerates with T_0. It is not only agreement with the predictions of theoretical calculations [46,47] but also with the experimental observations of thermally induced DW motion in nanowires
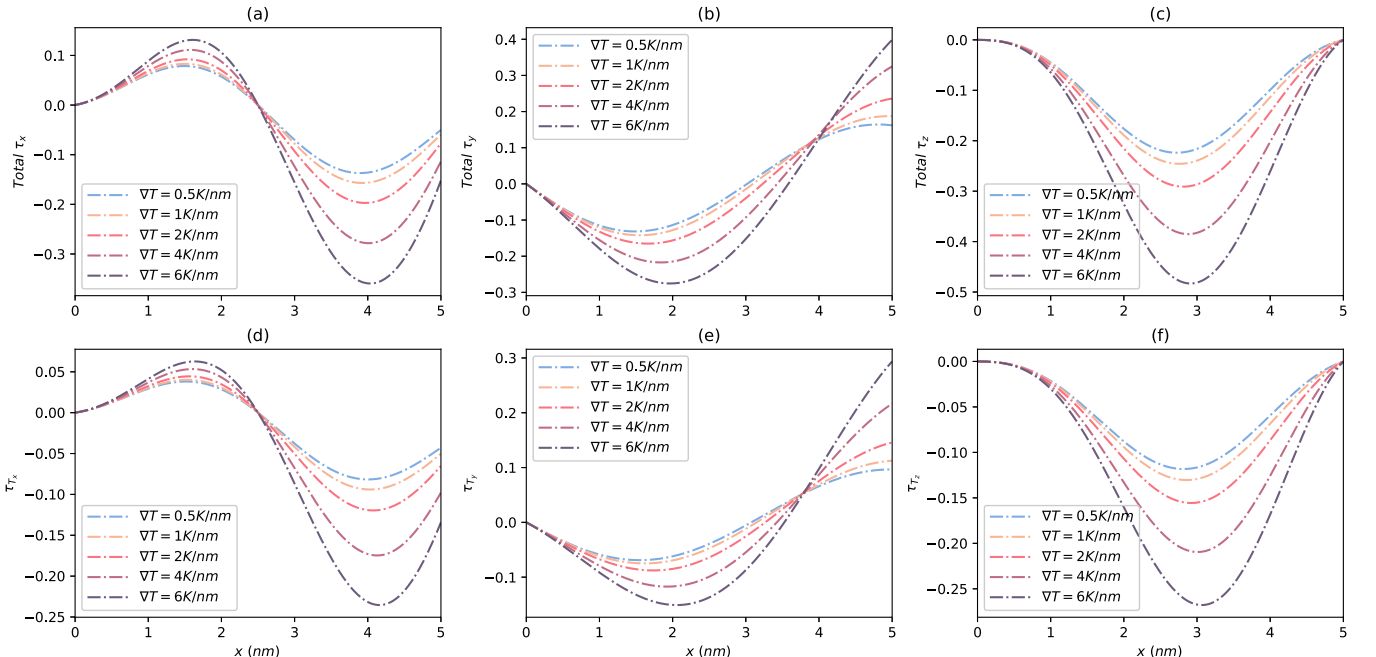

FIG. 4. (a), (b), (c) are the x, y, and z components of total spin torque $\boldsymbol{\tau}_{\text{total}}$ and (d), (e), (f) are the x, y, and z components of TSTT $\boldsymbol{\tau}_T$ versus position at different temperature gradients at $t = 0$.
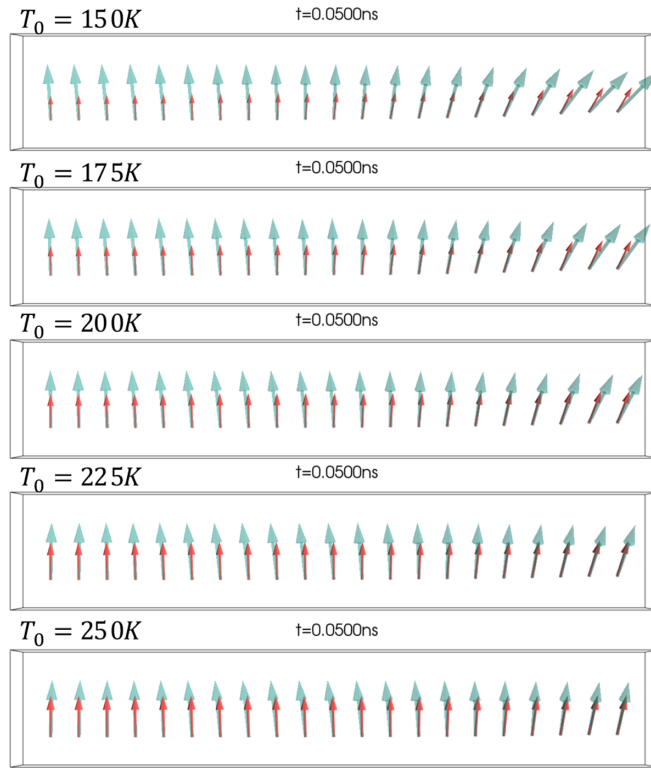
FIG. 5. The 3D vector diagram of magnetization $M(x, t)$ (marked by green arrow) and spin accumulation $m(x, t)$ (indicated by red arrow). The temperature gradients are taken as $\kappa = 2$ K/nm.

[48–51]. It should be pointed out that there are different views on how the thermodynamics participates in and assists the current-induced DW motion: the thermally reduction of de-pinning field and critical current density [46,50], the thermally reduction of saturation magnetization [48], the thermally reduction of magnetocrystalline anisotropy [52–54], and so on. In our theory, the thermally activated and assisted process is explained by the variation of spin accumulation and STT with temperature, as shown in Fig. 7.

The influence of different T_0 on TSTT τ_T and the total spin torque τ_{total} are demonstrated in Fig. 7, from which it can be seen that the amplitude of TSTT at the initial time increases with T_0, which also leads to the increase of the total

spin torque. It should be noted that, at first glance, Eq. (23) indicates that the TSTT is proportional to $\frac{1}{T}$, it means that the increase of temperature will lead to the decrease of the TSTT, which is contrast to the numerical result in Fig. 7. In fact, it can be explained as follows: As we know, only the electrons near Fermi energy E_F can participate in the transport; the increase of temperature will increase the number of thermally activated electrons that participate in the transport procedure, which means there are more electrons that will contribute to the transport procedure. According to the definitions of spin accumulation Eq. (12), total spin current density Eq. (13), and thermal spin current density Eq. (18), which are the integral of spinor distribution function over momentum p within the interval Δp, this will result in the increase of spin accumulation, the total spin torque, and TSTT, as shown in Fig. 7. Therefore, the Joule heating effect of spintronics devices can play a positive role in the operating efficiency.

IV. SUMMARY AND DISCUSSION

In the framework of the SBE, the temperature is introduced into the spinor distribution function by making a local equilibrium approximation, and the continuity Eq. (14) and the spin diffusion Eq. (15) satisfied by the spin accumulation $m(x, t)$ and spin current density $j_s(x, t)$ driven by external electric field E_x and temperature gradient ∇T are derived. In the relaxation time approximation, we solve the spin diffusion equation, and obtain the expression of spin accumulation $m(x)$ at the steady state. Substituting $m(x)$ into the definition of Levy's STT, we can get the analytical expression of the total spin torque τ_{total} Eq. (17), which contains both the ESTT and TSTT. Our expression of TSTT is derived analytically, which has different terms than Bauer's phenomenological TSTT. The first two terms in Eq. (22) correspond to Bauers's TSTT, which are induced by the temperature gradient, from which we can determine the spin conversion factor P' and the phenomenological coefficient β_Q in Bauer's expression theoretically, where we find that β_Q depends on the spin-flip relaxation time of electron and exchange coupling strength between itinerant electron and local magnetic moments; while the last two terms are caused by the inhomogeneity of magnetization in DWs, which depend on the temperature by the charge density. The analytical expression of TSTT Eq. (22) is our main result.
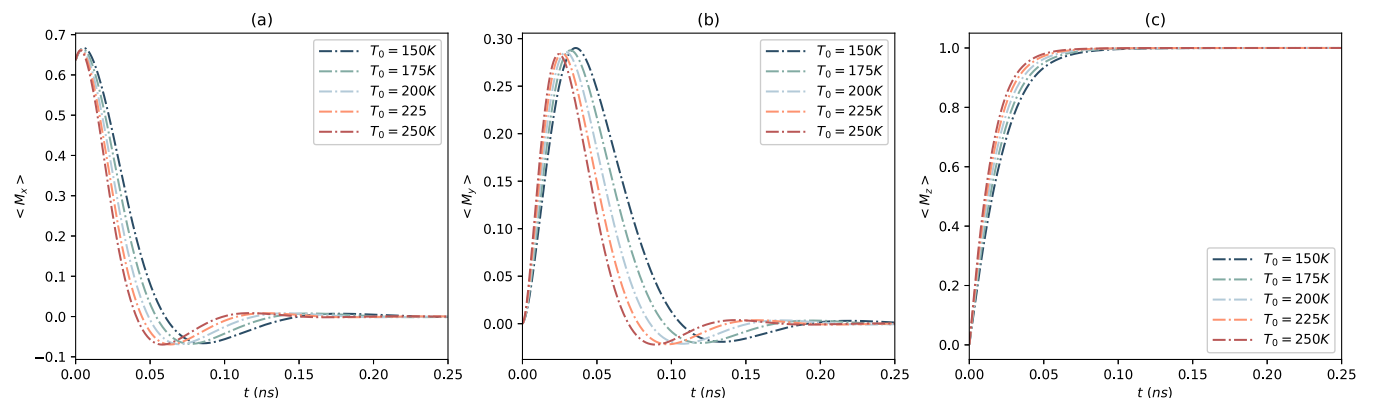

FIG. 6. The x, y, z components of the total magnetic moment $\langle M \rangle(t)$ at different temperatures versus time.
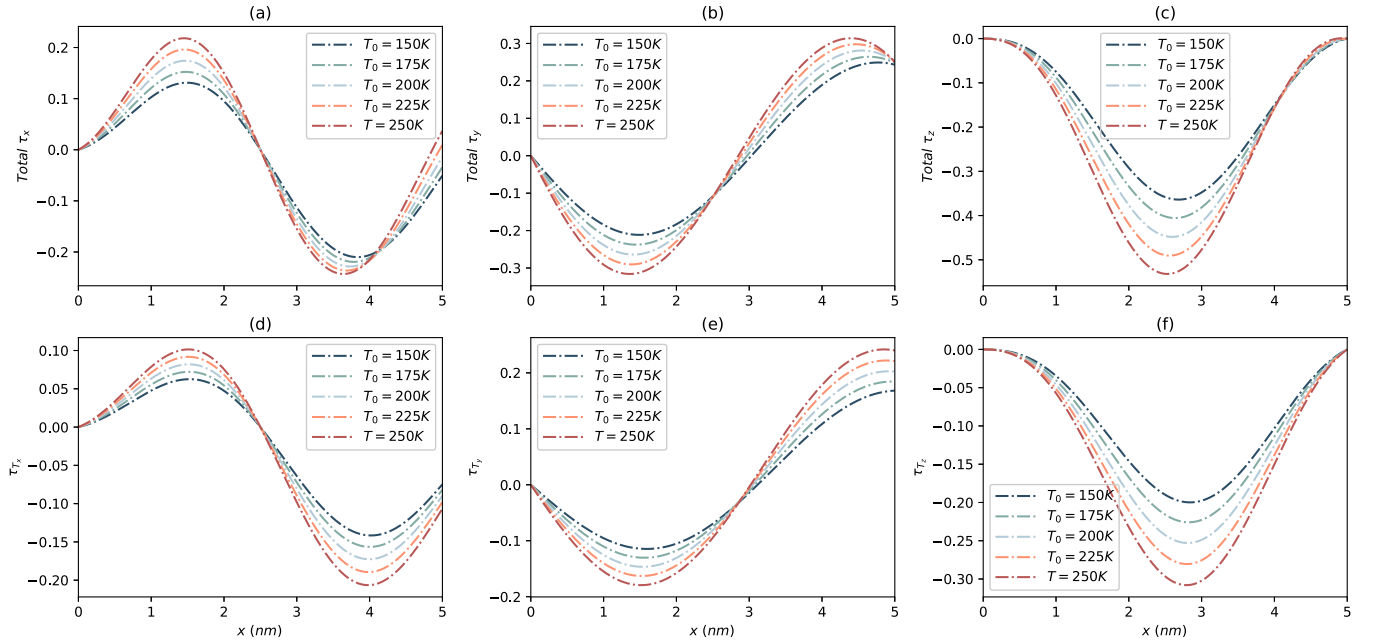
FIG. 7. (a), (b), (c) are the x, y, z components of total spin torque $\boldsymbol{\tau}_{\text{total}}$ and (d), (e), (f) are the x, y, z components of TSTT $\boldsymbol{\tau}_T$ versus position at different temperatures at $t = 0$.

By numerically solving the coupled equations SBE + LLGL Eqs. (5), (6), and (26), we investigate the magnetization dynamics at different temperature gradient ∇T and cold end temperature T_0 in a DW. We find (1) the velocity of the DW v_{DW} increases with temperature gradient ∇T at a fixed cold end temperature, because the TSTT is proportional to the ∇T, which drives the motion of the DW and (2) the v_{DW} increases with cold end temperature T_0 when we fix the temperature gradient ∇T. Although the TSTT appears to be proportional to $\frac{1}{T}$, the increase of T_0 leads to the increase of spin accumulation $\boldsymbol{m}(x)$ and the spin current density $\boldsymbol{j}_s(x)$, as well as total spin torque. The above conclusion is consistent with the experimental observations in Refs. [31,43,44,48–51].

APPENDIX: DERIVATION OF THE EXPRESSION OF SPIN ACCUMULATION AT STEADY-STATE EQ. (16)

In this Appendix, we will present the detailed derivation of Eq. (16). Substituting $n(x,t) = \frac{1}{2}n(x)[1 + \exp(-\frac{t}{\tau})]$, $\boldsymbol{m}(x,t) = \frac{1}{2}\boldsymbol{m}(x)[1 + \exp(-\frac{t}{\tau_s})]$, and $\boldsymbol{j}_s(x,t) = \frac{1}{2}\boldsymbol{j}_s(x)[1 + \exp(-\frac{t}{\tau_s})]$ into the spin diffusion Eq. (15), the spin diffusion equation under relaxation time approximation is

$$-\frac{1}{\tau_s}\exp\left(-\frac{t}{\tau_s}\right)\boldsymbol{m}(x) + \left[1 + \exp\left(-\frac{t}{\tau_s}\right)\right]\frac{\partial \boldsymbol{j}_s(x)}{\partial x}$$
$$= \left[1 + \exp\left(-\frac{t}{\tau_s}\right)\right]\left\{-\frac{\boldsymbol{m}(x) - \langle \boldsymbol{m}\rangle}{\tau_s} + \frac{J_{\text{ex}}}{\hbar}\boldsymbol{M} \times \boldsymbol{m}(x)\right\} + \left[1 + \exp\left(-\frac{t}{\tau}\right)\right]u_x\frac{\partial \boldsymbol{M}}{\partial x}n(x). \tag{A1}$$

When $t \gg \tau_s$, we can obtain the steady-state spin diffusion equation

$$\frac{\partial \boldsymbol{j}_s(x)}{\partial x} = -\frac{\boldsymbol{m}(x) - \langle \boldsymbol{m}\rangle}{\tau_s} + \frac{J_{\text{ex}}}{\hbar}\boldsymbol{M} \times \boldsymbol{m}(x) + u_x\frac{\partial \boldsymbol{M}}{\partial x}n(x), \tag{A2}$$

which can be rewritten as

$$\boldsymbol{m}(x) = -\tau_s\frac{\partial \boldsymbol{j}_s(x)}{\partial x} + \xi \boldsymbol{M} \times \boldsymbol{m}(x) + \tau_s u_x\frac{\partial \boldsymbol{M}}{\partial x}n(x) + \langle \boldsymbol{m}\rangle, \tag{A3}$$

where $\xi = \tau_s \frac{J_{ex}}{\hbar}$. To explore the expression of the steady-state spin accumulation $\boldsymbol{m}(x)$, we first multiply $\boldsymbol{M} \times$ on both sides of Eq. (A3),

$$\boldsymbol{M} \times \boldsymbol{m}(x) = -\tau_s \boldsymbol{M} \times \frac{\partial \boldsymbol{j}_s(x)}{\partial x} + \xi \boldsymbol{M} \times [\boldsymbol{M} \times \boldsymbol{m}(x)] + \tau_s u_x \boldsymbol{M} \times \frac{\partial \boldsymbol{M}}{\partial x} n(x) + \boldsymbol{M} \times \langle \boldsymbol{m} \rangle, \tag{A4}$$

where $\boldsymbol{M} \times \langle \boldsymbol{m} \rangle = 0$ because the equilibrium spin accumulation is always parallel to the magnetization. Equation (A4) can be expanded as

$$\boldsymbol{M} \times \boldsymbol{m}(x) = -\tau_s \boldsymbol{M} \times \frac{\partial \boldsymbol{j}_s(x)}{\partial x} + \tau_s u_x \boldsymbol{M} \times \frac{\partial \boldsymbol{M}}{\partial x} n(x) + \xi\{[\boldsymbol{M} \cdot \boldsymbol{m}(x)]\boldsymbol{M} - |\boldsymbol{M}|^2 \boldsymbol{m}(x)\}. \tag{A5}$$

Then, multiplying $\boldsymbol{M} \cdot$ on both sides of Eq. (A3),

$$\boldsymbol{M} \cdot \boldsymbol{m}(x) = -\tau_s \boldsymbol{M} \cdot \frac{\partial \boldsymbol{j}_s(x)}{\partial x} + \tau_s u_x \boldsymbol{M} \cdot \frac{\partial \boldsymbol{M}}{\partial x} n(x) + \boldsymbol{M} \cdot \langle \boldsymbol{m} \rangle. \tag{A6}$$

Inserting Eqs. (A5) and (A6) into Eq. (A3), the steady-state spin accumulation can be obtained as

$$\boldsymbol{m}(x) = \frac{1}{1+\xi^2}\left\{\langle \boldsymbol{m} \rangle + \xi^2 \boldsymbol{M}\left[\boldsymbol{M} \cdot \langle \boldsymbol{m} \rangle - \tau_s \boldsymbol{M} \cdot \frac{\partial \boldsymbol{j}_s(x)}{\partial x} + \tau_s u_x \boldsymbol{M} \cdot \frac{\partial \boldsymbol{M}}{\partial x} n(x)\right]\right\}$$
$$- \frac{\tau_s}{1+\xi^2}\left\{\frac{\partial \boldsymbol{j}_s(x)}{\partial x} + \xi \boldsymbol{M}\frac{\partial \boldsymbol{j}_s(x)}{\partial x} - u_x \frac{\partial \boldsymbol{M}}{\partial x} n(x) - \xi u_x \boldsymbol{M} \times \frac{\partial \boldsymbol{M}}{\partial x} n(x)\right\}, \tag{A7}$$

which is Eq. (16).

---

[1] M. N. Baibich, J. M. Broto, A. Fert, F. Nguyen Van Dau, F. Petroff, P. Etienne, G. Creuzet, A. Friederich, and J. Chazelas, Phys. Rev. Lett. **61**, 2472 (1988).

[2] J. Slonczewski, J. Magn. Magn. Mater. **159**, L1 (1996).

[3] L. Berger, Phys. Rev. B **54**, 9353 (1996).

[4] W. J. Gallagher and S. S. P. Parkin, IBM J. Res. Dev. **50**, 5 (2006).

[5] X. Han, X. Wang, C. Wan, G. Yu, and X. Lv, Appl. Phys. Lett. **118**, 120502 (2021).

[6] S. Aggarwal, H. Almasi, M. DeHerrera, B. Hughes, S. Ikegawa, J. Janesky, H. K. Lee, H. Lu, F. B. Mancoff, K. Nagel, G. Shimon, J. J. Sun, T. Andre, and S. M. Alam, in *Proceedings of the 2019 IEEE International Electron Devices Meeting (IEDM)* (IEEE, San Francisco, CA, 2019), pp. 2.1.1–2.1.4

[7] M. Natsui, A. Tamakoshi, H. Honjo, T. Watanabe, T. Nasuno, C. Zhang, T. Tanigawa, H. Inoue, M. Niwa, T. Yoshiduka, Y. Noguchi, M. Yasuhira, Y. Ma, H. Shen, S. Fukami, H. Sato, S. Ikeda, H. Ohno, T. Endoh, and T. Hanyu, in *Proceedings of the 2020 IEEE Symposium on VLSI Circuits* (IEEE, Honolulu, HI, 2020), pp. 1–2.

[8] W. C. Law and S. D. W. Wong, in *Emerging Non-volatile Memory Technologies: Physics, Engineering, and Applications*, edited by W. S. Lew, G. J. Lim, and P. A. Dananjaya (Springer Singapore, Singapore, 2021), pp. 45–102.

[9] C. Yang, Z. Wang, Q. Zheng, and G. Su, Eur. Phys. J. B **92**, 136 (2019).

[10] B. Jiang, D. Wu, Q. Zhao, K. Lou, Y. Zhao, Y. Zhou, C. Tian, and C. Bi, IEEE Electron Device Lett. **42**, 1766 (2021).

[11] B. K. Kaushik, S. Verma, A. A. Kulkarni, and S. Prajapati, in *Next Generation Spin Torque Memories* (Springer Singapore, Singapore, 2017), pp. 35–50.

[12] S. S. P. Parkin, M. Hayashi, and L. Thomas, Science **320**, 190 (2008).

[13] L. Thomas, S. H. Yang, K.-S. Ryu, B. Hughes, C. Rettner, D. S. Wang, C. H. Tsai, K. H. Shen, and S. S. Parkin, in *Proceedings of the 2011 International Electron Devices Meeting* (IEEE, Washington, DC, 2011), pp. 24.2.1–24.2.4.

[14] B. Göbel, A. F. Schäffer, J. Berakdar, I. Mertig, and S. S. P. Parkin, Sci. Rep. **9**, 12119 (2019).

[15] Y. Jiang, S. Abe, T. Ochiai, T. Nozaki, A. Hirohata, N. Tezuka, and K. Inomata, Phys. Rev. Lett. **92**, 167204 (2004).

[16] S. W. Jung, W. Kim, T. D. Lee, K. J. Lee, and H. W. Lee, Appl. Phys. Lett. **92**, 202508 (2008).

[17] O. Boulle, G. Malinowski, and M. Kläui, Mater. Sci. Eng.: R: Rep. **72**, 159 (2011).

[18] G. E. Bauer, E. Saitoh, and B. J. Van Wees, Nat. Mater. **11**, 391 (2012).

[19] M. Johnson and R. H. Silsbee, Phys. Rev. B **35**, 4959 (1987).

[20] Z. C. Wang, G. Su, and S. Gao, Phys. Rev. B **63**, 224419 (2001).

[21] K. Uchida, S. Takahashi, K. Harii, J. Ieda, W. Koshibae, K. Ando, S. Maekawa, and E. Saitoh, Nature (London) **455**, 778 (2008).

[22] J. C. Le Breton, S. Sharma, H. Saito, S. Yuasa, and R. Jansen, Nature (London) **475**, 82 (2011).

[23] M. Hatami, G. E. W. Bauer, Q. Zhang, and P. J. Kelly, Phys. Rev. Lett. **99**, 066603 (2007).

[24] T. T. Heikkilä, M. Hatami, and G. E. W. Bauer, Phys. Rev. B **81**, 100408(R) (2010).

[25] H. Yu, S. Granville, D. P. Yu, and J.-P. Ansermet, Phys. Rev. Lett. **104**, 146601 (2010).

[26] G. E. W. Bauer, S. Bretzel, A. Brataas, and Y. Tserkovnyak, Phys. Rev. B **81**, 024427 (2010).

[27] Z. Yuan, S. Wang, and K. Xia, Solid State Commun. **150**, 548 (2010).

[28] K. M. Hals, A. Brataas, and G. E. Bauer, Solid State Commun. **150**, 461 (2010).

[29] X. S. Wang and X. R. Wang, Phys. Rev. B **90**, 014414 (2014).

[30] M. T. Islam, X. S. Wang, and X. R. Wang, J. Phys.: Condens. Matter **31**, 455701 (2019).

[31] W. Jiang, P. Upadhyaya, Y. Fan, J. Zhao, M. Wang, L.-T. Chang, M. Lang, K. L. Wong, M. Lewis, Y.-T. Lin, J. Tang, S. Cherepov, X. Zhou, Y. Tserkovnyak, R. N. Schwartz, and K. L. Wang, Phys. Rev. Lett. **110**, 177202 (2013).

[32] A. Vansteenkiste, J. Leliaert, M. Dvornik, M. Helsen, F. Garcia-Sanchez, and B. Van Waeyenberge, AIP Adv. **4**, 107133 (2014).

[33] S. Zhang and Z. Li, Phys. Rev. Lett. **93**, 127204 (2004).

[34] A. Thiaville, Y. Nakatani, J. Miltat, and Y. Suzuki, Europhys. Lett. **69**, 990 (2005).

[35] Y. Tserkovnyak, A. Brataas, and G. E. Bauer, J. Magn. Magn. Mater. **320**, 1282 (2008).

[36] G. Tatara, H. Kohno, and J. Shibata, Phys. Rep. **468**, 213 (2008).

[37] Z.-C. Wang, Physica A **585**, 126404 (2022).

[38] J. Zhang, P. M. Levy, S. Zhang, and V. Antropov, Phys. Rev. Lett. **93**, 256602 (2004).

[39] A. Shpiro, P. M. Levy, and S. Zhang, Phys. Rev. B **67**, 104430 (2003).

[40] J. Zhang and P. M. Levy, Phys. Rev. B **71**, 184426 (2005).

[41] Z. Li and S. Zhang, Phys. Rev. Lett. **92**, 207203 (2004).

[42] See Supplemental Material at http://link.aps.org/supplemental/10.1103/PhysRevB.106.054432 for animated graphics showing magnetization and spin accumulation dynamics inside the domain wall at different temperature gradients and different temperatures.

[43] S. U. Jen and L. Berger, J. Appl. Phys. **53**, 2298 (1982).

[44] S. U. Jen and L. Berger, J. Appl. Phys. **59**, 1285 (1986).

[45] D. Hinzke and U. Nowak, Phys. Rev. Lett. **107**, 027205 (2011).

[46] S. Moretti, V. Raposo, and E. Martinez, J. Appl. Phys. **119**, 213902 (2016).

[47] J. Chico, C. Etz, L. Bergqvist, O. Eriksson, J. Fransson, A. Delin, and A. Bergman, Phys. Rev. B **90**, 014434 (2014).

[48] S. Emori, C. K. Umachi, D. C. Bono, and G. S. Beach, J. Magn. Magn. Mater. **378**, 98 (2015).

[49] S. DuttaGupta, S. Fukami, C. Zhang, H. Sato, M. Yamanouchi, F. Matsukura, and H. Ohno, Nat. Phys. **12**, 333 (2016).

[50] Y. Kurokawa, R. Yoshimura, S. Sumi, and H. Awano, AIP Adv. **7**, 035325 (2017).

[51] Y. Shiota, K. Noda, Y. Hirata, K. Kuwano, S. Funada, R. Hisatomi, T. Moriyama, M. Stebliy, A. V. Ognev, A. S. Samardak, and T. Ono, J. Magn. Magn. Mater. **553**, 169251 (2022).

[52] A. Sukhov, L. Chotorlishvili, A. Ernst, X. Zubizarreta, S. Ostanin, I. Mertig, E. K. U. Gross, and J. Berakdar, Sci. Rep. **6**, 24411 (2016).

[53] P. Chureemart, R. F. L. Evans, and R. W. Chantrell, Phys. Rev. B **83**, 184416 (2011).

[54] G. V. Astakhov, J. Schwittek, G. M. Schott, C. Gould, W. Ossau, K. Brunner, and L. W. Molenkamp, Phys. Rev. Lett. **106**, 037204 (2011).